DTU Library

Current-Induced Membrane Discharge

Andersen, Mathias Bækbo; van Soestbergen, M.; Mani, A.; Bruus, Henrik; Biesheuvel, P. M.; Bazant, M. Z.

[Link back to DTU Orbit](#)

Current-Induced Membrane Discharge

M. B. Andersen,[1,][*] M. van Soestbergen,[3,4] A. Mani,[2] H. Bruus,[1] P. M. Biesheuvel,[3,5] and M. Z. Bazant[6]

[1]*Department of Micro- and Nanotechnology, Technical University of Denmark, DTU Nanotech Building 345 East,*
DK-2800 Kongens Lyngby, Denmark
[2]*Department of Mechanical Engineering, Stanford University, Stanford, California 94305, USA*
[3]*Wetsus, Centre of Excellence for Sustainable Water Technology, Agora 1, 8934 CJ Leeuwarden, The Netherlands*
[4]*Department of Applied Physics, Eindhoven University of Technology, Den Dolech 2, 5612 AZ Eindhoven, The Netherlands*
[5]*Department of Environmental Technology, Wageningen University, Bornse Weilanden 9, 6708 WG Wageningen, The Netherlands*
[6]*Departments of Chemical Engineering and Mathematics, Massachusetts Institute of Technology,*
Cambridge, Massachusetts 02139, USA
(Received 29 February 2012; published 5 September 2012)

Possible mechanisms for overlimiting current (OLC) through aqueous ion-exchange membranes (exceeding diffusion limitation) have been debated for half a century. Flows consistent with electro-osmotic instability have recently been observed in microfluidic experiments, but the existing theory neglects chemical effects and remains to be quantitatively tested. Here, we show that charge regulation and water self-ionization can lead to OLC by ''current-induced membrane discharge'' (CIMD), even in the absence of fluid flow, in ion-exchange membranes much thicker than the local Debye screening length. Salt depletion leads to a large electric field resulting in a local pH shift within the membrane with the effect that the membrane discharges and loses its ion selectivity. Since salt co-ions, H^+ ions, and OH^- ions contribute to OLC, CIMD interferes with electrodialysis (salt counterion removal) but could be exploited for current-assisted ion exchange and pH control. CIMD also suppresses the extended space charge that leads to electro-osmotic instability, so it should be reconsidered in both models and experiments on OLC.

Selective ion transport across charged, water-filled membranes plays a major role in ion exchange and desalination [1,2], electrophysiology [3], fuel cells [4,5], and lab-on-a-chip devices [6–10], but is not yet fully understood. A long-standing open question has been to explain the experimentally observed overlimiting current (OLC), exceeding classical diffusion limitation [11]. Possible mechanisms include the role of electro-osmotic instability (EOI) and water splitting in the bulk solution [12–15], as well as surface conduction and electro-osmotic flow in microchannels [16]. Vortices consistent with EOI have recently been observed under OLC conditions [7,17,18], although the theory of Rubinstein and Zaltzman [19–21] remains to be tested quantitatively. The water splitting mechanism, either catalyzed by membrane surface groups or through the second Wien effect, has not yet been conclusively tied to OLC [15,22–27].

In this Letter, we propose a chemical mechanism for OLC, ''current-induced membrane discharge'' (CIMD), resulting from membrane (de)protonation and water self-ionization, even in the absence of fluid vortices due to EOI, in ion-exchange membranes much thicker than the Debye screening length. The amphoteric nature of the charge of ion-exchange membranes (i.e., sensitivity to pH and other stimuli) is well known [5,28–33], but not in response to a large applied current. The basic physics of CIMD is illustrated in Fig. 1 for an anion-exchange membrane. During OLC, a large electric field develops on the upstream, salt-depleted side of the membrane, which expels H^+ and attracts OH^-, which have an association equilibrium with the charged groups of the membrane, causing the membrane to lose its positive charge (effectively, to deprotonate, as we will consider below) thereby allowing salt co-ions to pass and producing large pH gradients. The upstream solution becomes more acidic (low pH), while the downstream, salt-enriched solution and the membrane become more basic (high pH).

The local charge of an aqueous membrane strongly depends on the local pH. In our examples below, we consider an anion-exchange membrane with fixed surface groups of volumetric concentration c_{mem}, which selectively allows negatively charged anions (counterions) to pass, while largely blocking cations (co-ions) [34]. Depending on pH $\approx p[H] = -\log_{10}(c_H)$, where c_H is the proton concentration (H^+ or H_3O^+) in M, the membrane can discharge (deprotonate):

$$\mathrm{R\,H^+} \xrightleftharpoons{K} \mathrm{R} + \mathrm{H^+}. \tag{1}$$

In terms of non-deprotonatable surface groups, such as quarternary amine groups in anion exchange membranes, the above reaction is equivalent to the OH^- association reaction: $R^+ + OH^- \rightleftharpoons ROH$. The ratio of product to reactant concentrations in equilibrium is the dissociation constant K in M ($pK = -\log_{10}K$). Assuming a classical Langmuir adsorption isotherm [28–32,35,36], the ionization degree of the membrane,
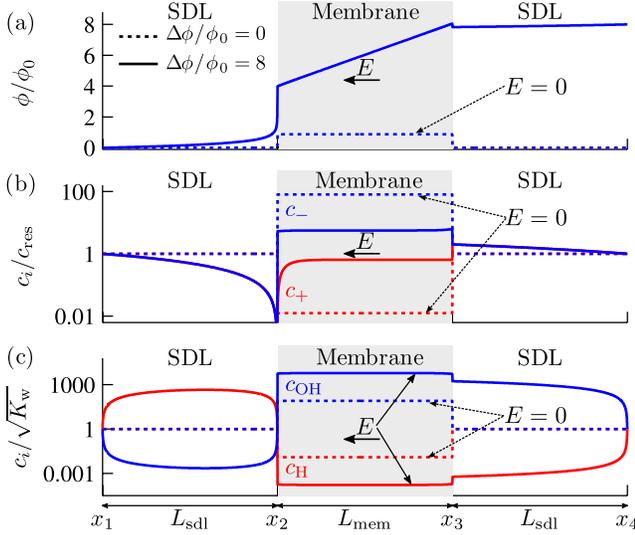
FIG. 1 (color online).   Basic physics of CIMD, illustrated by
numerical solutions of Eqs. (2), (5), and (6) for an anion
exchange membrane of thickness $L_{mem} = 100\ \mu m$ between
two stagnant diffusion layers (SDLs) each of thickness $L_{sdl} =$
$100\ \mu m$, both without ($E = 0$, dashed curves) and with ($E \neq 0$,
full curves) electric forcing for (a) electrostatic potential and
concentrations of (b) cations c_+ and anions c_- and (c) protons
c_H and hydroxyl ions c_{OH}.

$$\alpha = \left(1 + \frac{K}{c_H}\right)^{-1} = (1 + 10^{pH - pK})^{-1}, \qquad (2)$$

relates its charge concentration αc_{mem} to pH and pK. (For
a cation-exchange membrane, the power is $pK - pH$.)
To describe the local pH, we cannot assume Boltzmann
equilibrium with an external reservoir. Instead, we con-
sider ion transport coupled to membrane discharge Eq. (1)
and water self-ionization,

$$H_2O \overset{K_w}{\rightleftharpoons} OH^- + H^+, \qquad (3)$$
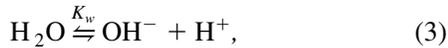
with dissociation constant

$$K_w = c_H c_{OH}, \qquad (4)$$

where $K_w = 10^{-14}\ M^2$ at $T = 25°C$. Although kinetics
can be included [5,24–26,37], the reactions (1) and (3)
are typically fast, so we assume local quasiequilibrium.

We now develop a membrane model (seemingly the
first) including all of these effects: (i) transport of four
ionic species, including co-ions and water ions (H^+
and OH^-) along with majority anions, (ii) water self-
ionization, and (iii) pH-dependent membrane charge.
We consider the prototypical 1D electrodialysis geometry
in Fig. 1, consisting of a planar ion-selective membrane
of thickness L_{mem} between two well-stirred reservoir com-
partments of salt ion concentration c_{res} and pH of pH_{res}.
We adopt the simplest and most commonly used model of
diffusion limitation [11], in which ion concentrations vary
across "stagnant diffusion layers" (SDLs) of thickness L_{sdl}

(of the order 10–100 μm) between the reservoirs and the
membrane, representing convection-diffusion boundary
layers.

Ionic diffusion, electromigration, and reactions are
described by four Nernst-Planck equations. Following
Refs. [28,29,38], we combine the Nernst-Planck equations
for H^+ and OH^- using Eq. (4) to eliminate the reaction
terms and relate the water-ion current density J_w to the
water-ion variable $P_w = (D_H c_H - D_{OH} c_{OH})/D_w$, in which
$D_w = \sqrt{D_H D_{OH}}$ is the geometric mean of the free H^+ and
OH^- diffusivities. We thus arrive at the following set of
coupled, nonlinear, differential equations to be solved in
both SDLs and the membrane [38]:

$$\frac{dJ_i}{dx} = 0, \qquad i = +, -, w, \qquad (5a)$$

$$J_\pm = \mp f_r D_\pm \left(\frac{dc_\pm}{dx} \pm c_\pm \frac{d\phi}{dx}\right), \qquad (5b)$$

$$J_w = -f_r D_w \left(\frac{dP_w}{dx} + [4K_w + P_w^2]^{1/2}\frac{d\phi}{dx}\right), \qquad (5c)$$

where J_i is the ionic current density of species i and f_r is a
correction factor for the ion diffusion coefficient in the
membrane, taking into account geometrical and chemical
effects which effectively retard ion transport ($f_r = 1$ in the
SDLs). Here, ϕ is the dimensionless mean electrostatic
potential scaled to the thermal voltage $V_T = k_B T/e =$
25.7 mV and satisfying Poisson's equation

$$\frac{d^2\phi}{dx^2} = -4\pi\lambda_B(\rho_{ions} + \rho_{mem}), \qquad (6)$$

where $\lambda_B = e^2/(4\pi\varepsilon_{r,j}\varepsilon_0 k_B T)$ is the Bjerrum length, and
$\rho_{ions} = \epsilon(c_+ - c_- + c_H - c_{OH})$ and $\rho_{mem} = \alpha\epsilon c_{mem}$ are
charge densities due to the ions and the immobilized
charges in the membrane, respectively. The porosity ϵ
of the membrane appears because concentrations c_i are
defined with respect to the interstitial, not total, volume
($\epsilon = 1$ in the SDLs). In our simulations below, we choose
the following typical parameters: $c_{mem} = 5$ M, $pK = 9.5$,
$L_{mem} = L_{sdl} = 100\ \mu m$, $\varepsilon_{r,sdl} = 78$, $\varepsilon_{r,mem} = 29$, $\epsilon = 0.4$,
$f_r = 0.02$ [39], $D_+ = 1.3 \times 10^{-9}\ m^2\,s^{-1}$ and $D_- =$
$2.0 \times 10^{-9}\ m^2\,s^{-1}$ (corresponding to NaCl), $D_H = 9.3 \times$
$10^{-9}\ m^2\,s^{-1}$, and $D_{OH} = 5.3 \times 10^{-9}\ m^2\,s^{-1}$. We also use
$pH_{res} = 7$ and $\beta = 2c_{res}/c_{mem} = 0.02$, unless otherwise
noted. The voltage difference across the system is $\Delta\phi$.
At the reservoir-SDL boundaries we set $c_\pm = c_{res}$ and
relate P_w to pH_{res}.

In spite of neglecting fluid flow, the model still predicts
OLC, as shown in Fig. 1. The classical ion concentration
polarization phenomenon is apparent in panel (b) with salt
depletion where counterions (anions) enter the membrane
($x = x_2$) and enrichment where they leave ($x = x_3$).
Within the membrane, however, anion depletion and cation
(co-ion) enrichment reveal a significant loss of selectivity
due to CIMD. At the same time, panel (c) shows large,
order-of-magnitude variations in c_H, "mirrored" by c_{OH}

through the equilibrium Eq. (4), with proton enrichment (acidity) in the left SDL and proton depletion (basicity) in both the membrane and the right SDL. The existence of such pH variations has been confirmed experimentally in similar systems [40–43].

Motivated by this observation, we analyze the pH gradients perturbatively in the full CIMD model. We consider underlimiting currents, assume thin, quasiequilibrium double layers (Donnan approximation) at the SDL-membrane interfaces, and solve the leading-order problem for c_+, c_- and ϕ with small perturbations in c_H and c_{OH}, valid when $(c_H + c_{OH})/(c_+ + c_-) \ll 1$. The resulting semianalytical model suffices to predict CIMD (variations of membrane charge with local pH) via Eq. (2). Numerical calculations show that pH and α are nearly constant across the membrane, so the water charge density is averaged between positions x_2 and x_3 (see below) to calculate the membrane charge and midplane pH [Fig. 2(b)] to be used in Eq. (2) to calculate α.

The final result for the most general model including membrane discharge, arbitrary values for pH_{res} and c_{res}, and the possibility that all diffusion coefficients are different, consists of Eq. (2) together with the set of algebraic equations below (see the Supplemental Material for details [44]). First, we introduce the dimensionless salt flux variable $j_{salt} = (J_- - J_+ D_-/D_+)/J_{lim}$, in which $J_{lim} = -2D_- c_{res}/L_{SDL}$ is the "classical" limiting current density [11], and obtain the salt current–voltage relation,

$$\Delta\phi = 4\tanh^{-1}(j_{salt}) + \frac{j_{salt}}{\gamma}\frac{\beta}{\alpha}, \qquad (7)$$

in which $\gamma = f_r/l_{mem}$, where $l_{mem} = L_{mem}/L_{sdl}$ is the membrane-to-SDL width ratio. The first term describes concentration polarization in the SDLs, while the second is the Ohmic response of the membrane. Next, we introduce the dimensionless water ion flux $j_w = J_w L_{sdl}/(D_w \sqrt{K_w})$ and water ion variable $\rho_w = P_w/\sqrt{K_w}$ and obtain the following equations: $\rho_w(x_3^{mem}) - \rho_w(x_2^{mem}) \times \exp[j_{salt}\beta/(\gamma\alpha)] + j_w/\gamma = 0$, $\sinh^{-1}[\rho_w(x_i^{mem})/2] = \sinh^{-1}[\rho_w(x_i^{sdl})/2] - \sinh^{-1}(\alpha/[\beta(1 \mp j_{salt})])$, and
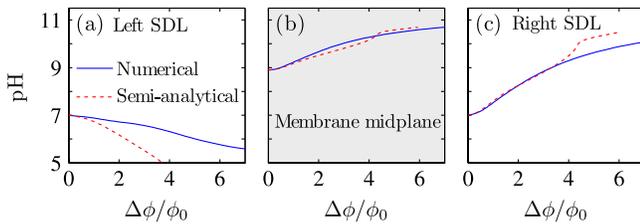

FIG. 2 (color online).   Predicted pH variations from the full numerical model, compared to the semianalytical approximation, as a function of the applied voltage (a) in the left SDL, just outside the local equilibrium screening layer on the membrane , (b) at the membrane midplane , and (c) in the right SDL, just outside the local equilibrium screening layer on the membrane.

$\rho_w(x_i^{sdl}) = \rho_w^{res} \mp j_w + \rho_0[1 + 2\gamma\beta/\alpha]\ln(1 \mp j_{salt})$, (where in these expressions $i = 2$ and 3 corresponds to $-$ and $+$, respectively). Here, ρ_w^{res} is related to pH_{res} and $\rho_0 = [4 + (\rho_w^{res})^2]^{(1/2)}$. Note that x_i^{mem} and x_i^{sdl} refer to positions on either side of the equilibrium electric double layer at the membrane–SDL interfaces. In the limit of an infinite membrane charge $\beta/\alpha \to 0$ the solution to the leading order problem [Eq. (7)] is simply the "classical" result [45], $j_{salt} = \tanh(\Delta\phi/4)$. We find the characteristic voltage factor ϕ_0 by expanding Eq. (7) for small $j_{salt} \ll 1$ and obtain $j_{salt} = \Delta\phi/\phi_0$ in which $\phi_0 = 4 + \beta/\gamma$ assuming constant $\alpha = 1$. The voltage factor ϕ_0 characterizes the exponential-like approach of the current density to its limiting value with applied voltage. Thus, in the classical picture, for $\Delta\phi/\phi_0 \approx 3$ we expect the current density to be at $\approx 95\%$ of its limiting value.

Results of the semianalytical model are compared with full numerical calculations in Fig. 2, which shows good agreement in the expected range of validity $\Delta\phi/\phi_0 \lesssim 1$. The pH appears to converge towards a limiting value for $\Delta\phi \to \infty$, and the jump in this limiting pH value between the left SDL and the membrane is huge, here about 5 pH units at the highest values of $\Delta\phi$ considered. We note that the deviation between the analytical and numerical solution is largest in the left SDL where electroneutrality is most strongly violated. This comparative analysis constitutes a validation of our numerics and provides further support for our conclusions regarding the role of pH in controlling the ionic transport properties of ion-selective membranes.

We now turn to a numerical analysis of the CIMD model Eqs. (2)–(6). For comparison, we also solve the classical model M_1 used in all prior work on EOI [17–21] in which (i) $c_+ = 0$ in the membrane, (ii) $c_H = c_{OH} = 0$ everywhere, and (iii) $\alpha = 1$ for all conditions. Additionally, we solve two intermediate models which include co-ions in the membrane with $\alpha = 1$ and either *exclude* (M_2) or *include* (M_4) water ions, i.e., taking 2 or 4 ions into account in the membrane, respectively. The total current density is $J_{tot} = J_+ + J_- + J_w$.

Figure 3(a) shows the significant decrease in the ionization degree α predicted by the CIMD model, in contrast to the constant $\alpha = 1$ in the M_1 model. Moreover, α decreases with decreasing β (due to the increasing Donnan potential) and decreases with pH_{res} (due to decreasing c_H in the membrane). A striking, and yet unexplained prediction is that for $\Delta\phi/\phi_0 \lesssim 3$ and pH_{res} larger than 7 the ionization degree is almost constant until the curve hits that for $pH_{res} = 7$ after which the curves follow each other. In general we find beyond a few times ϕ_0 that reservoir pH has a very small influence on membrane charge, fluxes, and currents [see also Figs. 3(b)–3(d)]. A more in-depth analysis of the effect of reservoir pH and the inclusion of additional chemical species is left for future work. Figure 3(b) shows the significant increase of co-ion flux J_+, thus loss
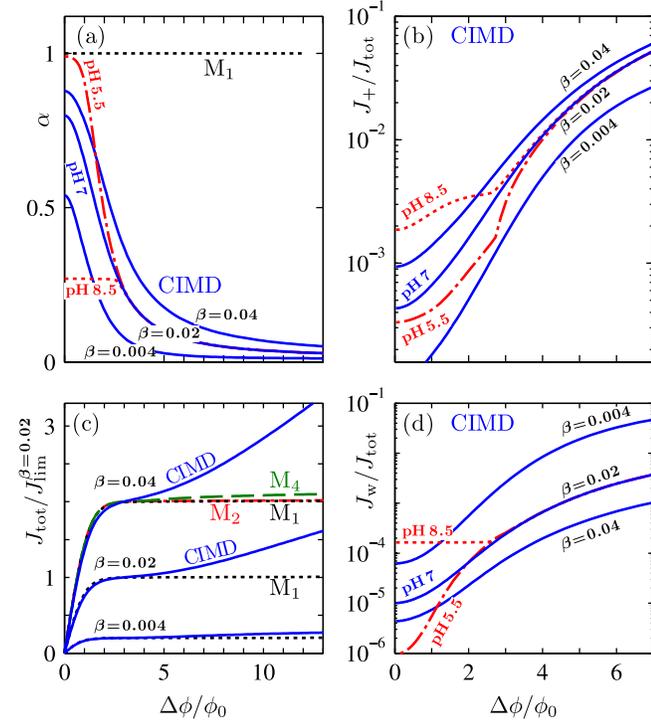
FIG. 3 (color online).   Comparison of the classical M_1 model (only counterions in the membrane) with the full CMID model for different concentration ratios $\beta = 2c_{res}/c_{mem} = 0.004, 0.02, 0.04$, and in the case $\beta = 0.02$ for pH$_{res} = 5.5, 7, 8.5$. (a) Membrane ionization degree α. (b) Co-ion current J_+. (c) Total current J_{tot}. (d) Water ion current J_w.
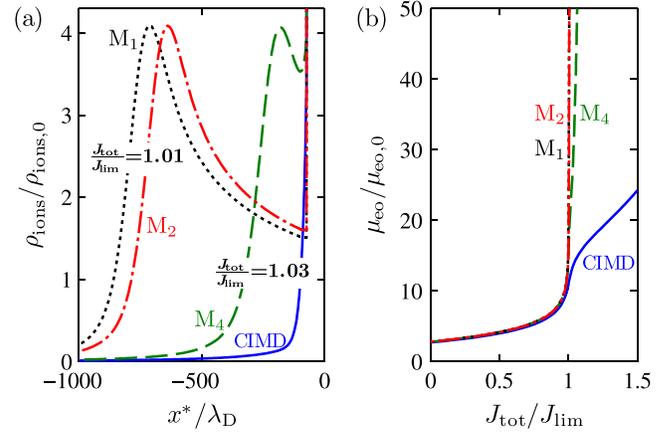

FIG. 4 (color online).   Comparison of three fixed-charge membrane models M_n having $n = 1, 2,$ or 4 mobile ionic species and the CIMD model for (a) charge density ρ_{ions} versus distance x^* from the membrane scaled to the reservoir Debye length λ_D, and (b) electro-osmotic mobility μ_{eo} as a function of total current J_{tot}. To further stress the effect of CIMD, the CIMD and M_4 models are shown for the higher current density $J_{tot}/J_{lim} = 1.03$ compared to $J_{tot}/J_{lim} = 1.01$ for the M_1 and M_2 models.

of membrane selectivity, with increasing voltage, as predicted by the CIMD model, for all values of pH and β, while Fig. 3(d) shows likewise the increase in current density J_w due to water ions. Still, these contributions do not sum to the increased current during OLC, as shown in Fig. 3(c), the difference being due to increased counterion flux J_-.

Although the current–voltage relation in CIMD is quite complicated, our simulations and analysis suggest two general trends: (i) OLC increases with reservoir salt concentration, roughly as $\beta^{0.65}$ for the parameters of Fig. 3; (ii) OLC is nearly independent of reservoir pH, in spite of the large pH gradients produced across the membrane.

Finally, we analyze the possible effect of CIMD on EOI. In the classical M_1 model, nonequilibrium space charge forms at the limiting current [45–48], and its growing separation from the membrane reduces viscous resistance to electro-osmotic flow and destabilizes the fluid [19–21]. As a measure of the propensity to develop EOI we use the transverse (Helmholtz-Smoluchowski) electro-osmotic mobility $\mu_{eo}/\mu_{eo,0}$ at the left SDL-reservoir edge, which is equal to the first moment of the charge density, $-4\pi\lambda_B \int_{x_1}^{x_2} x\rho_{ions}dx$, or the dimensionless potential difference across the left SDL, $\phi(x_1) - \phi(x_2)$.

Figure 4(a) shows that slightly above the limiting current ($J_{tot}/J_{lim} = 1.01$) the M_1 model already predicts a very significant extended space charge layer (the "shoulder" maximum in $\rho_{ions}/\rho_{ions,0} = (\lambda_D L_{SDL}/\phi_0)d^2\phi/dx^2$ several hundred Debye lengths from the membrane), whereas for an even higher current ($J_{tot}/J_{lim} = 1.03$), using the more realistic CIMD model, the extension of this layer is still very minor. The two intermediate models lie in between. Figure 4(b) shows how the transverse electro-osmotic mobility is predicted by the M_1 model to diverge at the limiting current. This divergence is significantly reduced only by the full CIMD model including simultaneously co-ion access, water ion transport, water splitting, and membrane discharge. We note that a proper analysis of EOI would be more involved, since here we have simply focused on the transverse electro-osmotic mobility as a way of illustrating the suppression of EOI due to CIMD.

In conclusion, we have theoretically demonstrated that OLC through aqueous ion-exchange membranes can result from CIMD, or loss of ion selectivity due to (de-) protonation coupled to ion transport and water self-ionization. The appearance of OLC carried partially by salt co-ions and water ions reduces separation efficiency in electrodialysis, but the associated large pH gradients and membrane discharge could be exploited for current-assisted ion exchange or pH control. In addition to the effect of the water ions, the loss of ion selectivity due to CIMD leads to a further suppression of the nonequilibrium space charge that is much larger than in any of the models M_1, M_2, and M_4, see Fig. 4(a). The nonequilibrium space charge is responsible for EOI and thus CIMD should be considered in both models and experiments on OLC with

fluid flow. Although we have developed the theory for ion-exchange membranes in aqueous solutions, CIMD could occur in any nanofluidic system with an electrolyte whose ions regulate the surface charge.

———————————

*Present address: Department of Mechanical Engineering, Stanford University, Stanford, California 94305, USA

[1] F. Helfferich, *Ion Exchange* (Dover, New York, 1995).
[2] X. Tongwen, J. Membr. Sci. **263**, 1 (2005).
[3] T. F. Weiss, *Cellular Biophysics* (MIT Press, Cambridge, MA, 1996).
[4] R. P. O'Hare, S.-W. Cha, W. G. Colella, and F. B. Prinz, *Fuel Cell Fundamentals* (Wiley, New York, 2009).
[5] P. Berg, K. Promislow, J. S. Pierre, J. Stumper, and B. Wetton, J. Electrochem. Soc. **151**, A341 (2004).
[6] Y.-C. Wang, A. L. Stevens, and J. Han, Anal. Chem. **77**, 4293 (2005).
[7] S. J. Kim, Y.-C. Wang, J. H. Lee, H. Jang, and J. Han, Phys. Rev. Lett. **99**, 044501 (2007).
[8] R. Schoch, J. Han, and P. Renaud, Rev. Mod. Phys. **80**, 839 (2008).
[9] W. Sparreboom, A. van den Berg, and J. C. T. Eijkel, Nature Nanotech. **4**, 713 (2009).
[10] S. J. Kim, S. H. Ko, K. H. Kang, and J. Han, Nature Nanotech. **5**, 297 (2010).
[11] V. G. Levich, *Physicochemical Hydrodynamics* (Prentice-Hall, New York, 1962).
[12] Y. Fang, Q. Li, and M. E. Green, J. Colloid Interface Sci. **86**, 185 (1982).
[13] V. Zabolotsky, V. Nikonenko, N. Pismenskaya, E. Laktionov, M. Urtenov, H. Strathmann, M. Wessling, and G. Koops, Sep. Purif. Technol. **14**, 255 (1998).
[14] V. V. Nikonenko, N. D. Pismenskaya, E. I. Belova, P. Sistat, P. Huguet, G. Pourcelly, and C. Larchet, Adv. Colloid Interface Sci. **160**, 101 (2010).
[15] L.-J. Cheng and H.-C. Chang, Biomicrofluidics **5**, 046502 (2011).
[16] E. V. Dydek, B. Zaltzman, I. Rubinstein, D. S. Deng, A. Mani, and M. Z. Bazant, Phys. Rev. Lett. **107**, 118301 (2011).
[17] S. M. Rubinstein, G. Manukyan, A. Staicu, I. Rubinstein, B. Zaltzman, R. G. H. Lammertink, F. Mugele, and M. Wessling, Phys. Rev. Lett. **101**, 236101 (2008).
[18] G. Yossifon and H.-C. Chang, Phys. Rev. Lett. **101**, 254501 (2008).
[19] I. Rubinstein and B. Zaltzman, Phys. Rev. E **62**, 2238 (2000).
[20] I. Rubinstein, B. Zaltzman, J. Pretz, and C. Linder, Russ. J. Electrochem. **38**, 853 (2002).
[21] B. Zaltzman and I. Rubinstein, J. Fluid Mech. **579**, 173 (2007).
[22] K. Spiegler, Desalination **9**, 367 (1971).
[23] C. Forgacs, N. Ishibashi, J. Leibovitz, J. Sinkovic, and K. Spiegler, Desalination **10**, 181 (1972).
[24] R. Simons, Nature (London) **280**, 824 (1979).
[25] R. Simons, Electrochim. Acta **29**, 151 (1984).
[26] C.-O. Danielsson, A. Dahlkild, A. Velin, and M. Behm, Electrochim. Acta **54**, 2983 (2009).
[27] Y. Tanaka, J. Membr. Sci. **350**, 347 (2010).
[28] P. Ramirez, A. Alcaraz, and S. Mafé, J. Electroanal. Chem. **436**, 119 (1997).
[29] P. Ramirez, S. Mafé, A. Tanioka, and K. Saito, Polymer **38**, 4931 (1997).
[30] W. B. S. de Lint, P. M. Biesheuvel, and H. Verweij, J. Colloid Interface Sci. **251**, 131 (2002).
[31] R. Takagi and M. Nakagaki, Sep. Purif. Technol. **32**, 65 (2003).
[32] S. Bandini, J. Membr. Sci. **264**, 75 (2005).
[33] K. L. Jensen, J. T. Kristensen, A. M. Crumrine, M. B. Andersen, H. Bruus, and S. Pennathur, Phys. Rev. E **83**, 056307 (2011).
[34] A. Yaroshchuk, J. Membr. Sci. **396**, 43 (2012).
[35] K. Köhler, P. M. Biesheuvel, R. Weinkamer, H. Möhwald, and G. B. Sukhorukov, Phys. Rev. Lett. **97**, 188301 (2006).
[36] P. M. Biesheuvel, T. Mauser, G. B. Sukhorukov, and H. Möhwald, Macromolecules **39**, 8480 (2006).
[37] P. M. Biesheuvel, Langmuir **18**, 5566 (2002).
[38] M. Van Soestbergen, A. Mavinkurve, R. T. H. Rongen, K. M. B. Jansen, L. J. Ernst, and G. Q. Zhang, Electrochim. Acta **55**, 5459 (2010).
[39] A. Elattar, A. Elmidaoui, N. Pismenskaia, C. Gavach, and G. Pourcelly, J. Membr. Sci. **143**, 249 (1998).
[40] A. P. Thoma, A. Viviani-Nauer, S. Arvanitis, W. E. Morf, and W. Simon, Anal. Chem. **49**, 1567 (1977).
[41] L. Jialin, W. Yazhen, Y. Changying, L. Guangdou, and S. Hong, J. Membr. Sci. **147**, 247 (1998).
[42] J. J. Krol, M. Wessling, and H. Strathmann, J. Membr. Sci. **162**, 145 (1999).
[43] J.-H. Choi, H.-J. Lee, and S.-H. Moon, J. Colloid Interface Sci. **238**, 188 (2001).
[44] See Supplemental Material at http://link.aps.org/supplemental/10.1103/PhysRevLett.109.108301 for more details regarding the derivation of the model equations and the semi-analytical model.
[45] M. Z. Bazant, K. T. Chu, and B. J. Bayly, SIAM J. Appl. Math. **65**, 1463 (2005).
[46] I. Rubinstein and L. Shtilman, J. Chem. Soc., Faraday Trans. 2 **75**, 231 (1979).
[47] K. T. Chu and M. Z. Bazant, SIAM J. Appl. Math. **65**, 1485 (2005).
[48] P. M. Biesheuvel, M. van Soestbergen, and M. Z. Bazant, Electrochim. Acta **54**, 4857 (2009).